NUCL SCI TECH (2016) 27:69
DOI 10.1007/s41365-016-0066-x

Characterization of the copper-containing amine oxidase from *Trifolium pratense* seedlings

Yong-Ming Zhang[1] · Guo-Long Li[2] · Rui-Bo Zhong[3] · Yu-Xing Ma[3] · Pei Gong[3] · Feng Zhang[3]

Received: 23 August 2015 / Revised: 26 October 2015 / Accepted: 2 November 2015 / Published online: 12 May 2016

Abstract We studied the kinetic characterizations of the *Trifolium pratense* seedlings copper-containing amine oxidase (TPAO) by using various amine-containing substrates. The catalyzing rate for all of amine-containing substrates can be ordered as diamines > polyamines > aromatic monoamines, and it shows an apparent trend in each category of substrates such as the longer the carbon chain, the lower the V_{max} is, so does the V_{max}/K_m values but is opposite for the K_m value of TPAO. The distinct differences between the kinetic parameters for different amine-containing substrates indicated that the rate-determining step of the catalytic reaction strongly depends on the substrate's chemical structure. It is concluded that both pH and ionic strength can affect the catalytic activity of TPAO via influencing the coulomb interaction-mediated enzyme–substrate docking processes, which can be attributed to the potential of charged groups from both substrates and the activity sites of TPAO by the regulation of ionic strength.

Keywords Amineoxidase · *Trifolium pretense* · Kinetic characterization · pH dependence · Ionic strength

1 Introduction

Amine oxidases (AOs) catalyze the oxidative deamination of polyamines which are ubiquitous polycationic compounds involved in many significant events of the cell cycles [1]. The amine oxidases can be classified into two categories: copper-containing amine oxidases (CuAOs; EC1.4.3.6) and flavin-containing polyamine oxidases (PAOs; EC1.5.3.11). CuAOs are a ubiquitous and novel group of quinoenzymes that catalyze the oxidation of aromatic and aliphatic primary amines to be corresponding aldehydes with concomitant reduction in molecular oxygen to hydrogen peroxide [2], which can be concluded as following reaction formula (in which R represents aromatic or aliphatic moieties):

$$\begin{aligned} &R - CH_2 - NH_2 + H_2O + O_2 \\ &\quad \rightarrow R - CHO + NH_3 + H_2O_2 \end{aligned} \quad (1)$$

Diamines like putrescine and cadaverine can be oxidized by monoamine or polyamine AOs with a low catalytic activity; however, they have been considered preferred substrates for the characterization of CuAOs in plants [3]. CuAOs can be highly purified and characterized from a

This study was supported by the Department of Education of Inner Mongolia and Inner Mongolia Natural Science Foundation of China for Basic Research (No. NJZY13054), the National Natural Science Foundation of China (Nos. 31360214, 21171086 and 81160213), the Inner Mongolia Autonomous Region Science and Technology Department (No. 211-202077), the Inner Mongolia Grassland Talent (No. 108-108038), the Natural Science Foundation of Inner Mongolia Autonomous Region of China (Nos. 2013MS1121 and 2015MS0806) and the Inner Mongolia Agricultural University (Nos. 109-108040, 211-109003 and 211-206038).

✉ Yong-Ming Zhang
abel518@hotmail.com

✉ Feng Zhang
fengzhang1978@hotmail.com

[1] College of Life Science and Technology, Inner Mongolia Normal University, Hohhot 010022, China

[2] Sugar beet Physiological Institute, Inner Mongolia Agricultural University, Hohhot 010019, China

[3] Agricultrual Nanocenter, School of Life Sciences, Inner Mongolia Agricultural University, Hohhot 010018, China

variety of microorganisms including fungi and bacteria [4]. In plants, CuAOs have been detected in many species and particularly have higher levels when observing dicotyledons [5]. Some of them such as *Lens esculenta* [3], *Pisum sativum* [6], *Triticum aestivum* [7], *Euphorbia characias* [8] and *Vigna radiate* [9] have been highly purified and characterized. At this point in time, the kinetic mechanism of CuAOs in plants is not well understood, although it has been extensively studied [10–14]. The biological role of AOs has been reported mainly on the production of polyamine catabolism in hydrogen peroxide. Several extensive reviews have been recently published [1, 15–17].

In this article, we have thoroughly studied the kinetic characteristics of *Trifolium pratense* seedlings amine oxidase (TPAO) with using 8 different kinds of amine-containing substrates under different pH and ionic strengths. We have intensively discussed the catalyzing mechanism of TPAO for different amine derivatives and the effects of both pH and ionic strength.

2 Experimental section

2.1 Chemicals and materials

All chemicals were of the analytical grade and used without further purification. All of amine substrates were purchased from Sigma-Aldrich (Biodee, Beijing, China). *N*-ethyl-*N*-(2-hydroxy-3-sulfopropyl)-3-methylamine was a gift from Dojin Laboratories (Kumamoto, Japan). Horseradish peroxidase was purchased from Wako Pure Chemical (Osaka, Japan). Red clover (*T. pratense* L.) seeds were sterilized with 0.1 % benzalkonium chloride, thoroughly soaked with tap water for 8 h, and grown on moist filter paper (Whatman No. 1) for 10 days at 25 °C in total darkness. After treatments, the etiolated seedlings were harvested, frozen in liquid nitrogen and stored at −80 °C until use. The HPLC data were collected with a Hitachi Chromaster system. Spectrophotometric measurements were taken with a Hitachi UV-2800 instrument (Hitachi Co., Tokyo, Japan).

2.2 Enzyme purification and copper determination

Purified clover leaf seedlings containing amine oxidase were prepared as reported by Emmanuel Delhaize and John Webb [18]. Briefly, a six-step purification procedure has been adopted in the present investigation for purification of TPAO from 72-h germinated clover leaf seedlings. All the operations were carried out at 4 °C. Step 1: Clover leaf seedlings were homogenized in sodium phosphate buffer (10 mM, pH 7.5). The homogenate was filtered through cheesecloth and centrifuged at 10,000 g for 20 min. Step 2: The crude extract was subjected to $(NH_4)_2SO_4$ fractionation, and the protein precipitating at 35–65 % saturation was dispersed in sodium phosphate buffer (10 mM, pH 7.5) and dialyzed against the same buffer for 24 h [$(NH_4)_2SO_4$ fraction]. Step 3: The dialyzed fraction was then precipitated with precooled (−20 °C) acetone (Me_2CO, 50 mL/100 mL enzyme solution) with stirring and centrifuged at 15,000*g* for 20 min. Further Me_2CO at −20 °C was added (150 mL/100 mL enzyme solution) in the same manner, and the precipitation recovered by centrifugation at 20,000*g* for 30 min was dissolved in sodium phosphate buffer (10 mM, pH 7.5), dialyzed and centrifuged at 5000*g* for 5 min (Me_2CO fraction). Step 4: The Me_2CO fraction was applied to a DEAE-cellulose column (25 cm × 2.2 cm) previously equilibrated with sodium phosphate buffer (0.1 M, pH 7.5), and the column was washed with 200 mL of the same buffer. The enzyme fractions were eluted from the column with 0.1 M sodium phosphate buffer containing 0.2 M NaCl. The active fractions were pooled, brought to 70 % $(NH_4)_2SO_4$ saturation, and centrifuged at 10,000*g* for 20 min, and the precipitation was dissolved in 10 mM sodium phosphate buffer and dialyzed. Step 5: The dialyzed enzyme fraction (10 mL) was passed through the DEAE-Sephadex (A-25)column (33 cm × 1.8 cm) equilibrated with sodium phosphate buffer (0.1 M, pH 7.5), and inactive protein was washed from the column with sodium phosphate buffer containing 0.1 M NaCl. The enzyme was then eluted from the column with 0.3 M NaCl in sodium phosphate buffer (0.1 M, pH 7.5), precipitated with 70 % $(NH_4)_2SO_4$, centrifuged at 10,000*g* for 20 min, dissolved in 10 mM sodium phosphate buffer and dialyzed overnight. Step 6: The column (4 cm × 2 cm) of hydroxylapatite was equilibrated with sodium phosphate buffer (0.1 M, pH 7.5). The enzyme fraction obtained in step 5 was passed through the column, and the column was washed with the same buffer, and then, the enzyme was eluted with sodium phosphate buffer (0.3 M, pH 7.5).

Copper contents were determined by atomic absorption using an IL 951 atomic absorption spectrometer (Instrumentation Laboratory, Wilmington, DE). The spectral line was chosen 324.7 nm for copper.

2.3 Measurements of enzyme activity

The hydrogen peroxide-producing amine oxidase activity was continuously monitored by spectrophotometric detection in a reaction mixture with using the modified quinoneimine dye method that, in a previous report, we discussed using the purification of a novel FAD-dependent amine oxidase from oat seedlings [19]. The mixture for a standard assay contained 50 mM potassium phosphate buffer (pH 7.0), 0.5 mM *N*-ethyl-*N*-(2-hydroxy-3-sulfopropyl)-3-methylamine, 0.5 mM

4-aminoantipyrine, 3.3 purpurogallin units horseradish peroxidase, and enzyme solution in a total volume of 3.0 mL. The reaction was initiated with the addition of amine. The mixture was incubated at 37 °C, and the enzyme activity was determined by the absorbance at 555 nm.

Enzyme stability, as a function of pH, was determined in air-saturated solutions at 37 °C in the assay mixture including each of the following buffers: 50 mM acetate buffer, 100 mM K-phosphate buffer, 50 mM Tris–HCl buffer or 50 mM glycine-NaOH buffer. The pH was adjusted to the desired range (4.0–9.5) with the addition of NaOH or HCl.

Enzyme activity measurements, as a function of ionic strength, were taken in air-saturated solutions at 37 °C in the presence of 0.1 mM EDTA. The concentrated NaCl solutions were mixed with different amines as substrates. Controlled experiments without NaCl were performed throughout the entire experiment.

2.4 Analysis of kinetic parameters

K_m and V_{max} values were obtained by fitting the kinetic data to the Michaelis–Menten equation (Eq. 2) by nonlinear regression analysis using Microcal Origin 4.1 software and assuming a TPAO molecular weight of 150 kDa [18].

$$v = V_{max}[S]/(K_m + [S]) \quad (2)$$

The data reported account for the average of three experiments by using at least six amine concentrations each. The standard deviation was about ten percent of the measured value.

Kinetic parameters k_{cat} and k_{cat}/K_m values were graphically plotted against the proton concentration and fitted to an equation (Eq. 3) that determined measurements of enzyme stability as a function of pH [20].

$$y = y_0/(1 + [H^+]/K_{a1} + K_{a2}/[H^+]), \quad (3)$$

where K_{a1} and K_{a2} are the dissociation constant of protonated groups that control the dependence of kinetic parameters on pH and y_0 is the pH independent value of the parameter y (k_{cat} or k_{cat}/K_m) [21].

The kinetic data, V_{max} or V_{max}/K_m, on ionic strength (I) at pH 7.0 at 37 °C, were analyzed according to the Debye–Huckel equation (Eq. 4) [22]:

$$\log K_m = \log k_0 + 2CZ_aZ_bI^{1/2}, \quad (4)$$

where Z_a and Z_b are the charges of the species involved in the formation of activated complex, k_0 is the kinetic rate constant, K_m, at $I = 0$ and the constant C is 0.518 $M^{1/2}$ for a reaction occurring in water at 37 °C.

3 Results

3.1 Substrate specificity

The atomic absorption measurements have proved that the purified TPAO was one of the typical copper-containing AOs (data not shown). In order to characterize the substrate specificity of TPAO, different amine derivatives (Fig. 1) were used as the enzymatic substrates. The steady-state kinetic parameters for the oxidation reaction catalyzed by TPAO are summarized in Table 1. The V_{max} values of the analyzed substrates show distinct differences. The highest value of V_{max} in putrescine is 251 μM min^{-1} - mg^{-1}, which is approximately 14-fold as that of tyramine (18 μM min^{-1} mg^{-1}). All of amine-containing substrates can be ordered as diamines > polyamines > aromatic monoamines, and in each category of substrates, it shows an apparent trend as the longer the carbon chain, the lower the V_{max} is, which is also same as the V_{max}/K_m values but is opposite for the K_m value of TPAO, in that the highest K_m value of aromatic monoamines shows approximately 2 orders of magnitude higher than that of diamines. The distinct differences between the kinetic parameters for different amine-containing substrates indicated that the catalyzing activity of TPAO depends on the molecular

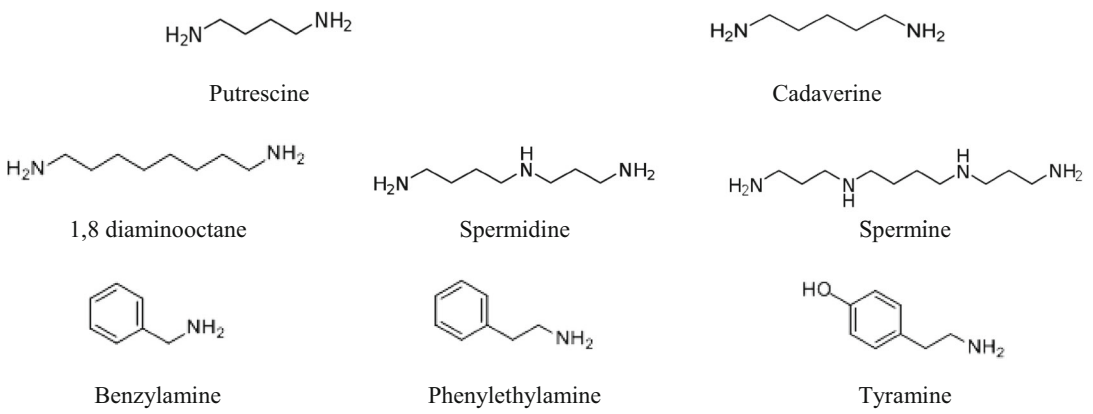

Fig. 1 Molecular structures of different amines used as substrates of TPAO

Table 1 Kinetic parameters of TPAO catalyzing different amine-containing substrates

Substrate	V_{max} (μM min^{-1} mg^{-1})	K_m (μM)	V_{max}/K_m (min^{-1} mg^{-1})
Putrescine	252	38	6.632
Cadaverine	197	89	2.213
1,8-Diaminooctane	122	196	0.622
Spermidine	98	348	0.282
Spermine	63	698	0.090
Benzylamine	46	2380	0.019
Phenylethylamine	18	3750	0.005
Tyramine	41	1920	0.021
Propylamine	n.d.*	n.d.	n.d.
Hexylamine	n.d.	n.d.	n.d.

All of the kinetic measurements are taken in standard assay mixture as described in the materials and methods at pH 7.0 and 37 °C. All the sets of measurements are run in triplicate

* n.d. means the sample is not detectable due to the too low readout

structure of its substrates. Both terminals of the spermidine molecule contain an amino-butyl end, so its structure is rather similar to putrescine. Other groups like phenyl and hydroxyl groups also show different influences on the catalytic efficiency of TPAO; for example, the V_{max}/K_m value for tyramine is much larger than both phenylethylamine and benzylamine.

3.2 pH dependence of catalytic parameters

To deepen the understanding the pH effect on the catalytic activity of TPAO, a pH ranging from 4.0 to 9.5 was chosen to this end. An asymmetrical bell-shaped curve obtained by plotting k_{cat} against pH (Fig. 2), from which the k_{cat} values for diamines are highest compared to polyamines and aromatic monoamines. The maximum peaks of the curves for putrescine and cadaverine are found around neutral pH; however, others are centered at alkaline region. As we know, the pH effect on the catalyzing activity is caused by protonation/deprotonation of the corresponding protonated groups, and it can be well described as the apparent pK_a values which can be calculated by fitting the data to Eq. 3. The pK_a values for different amine-containing substrates in the TPAO catalyzing reactions are summarized in Table 2, from which we can figure out that the pK_a values also show an increasing trend as the sequence for K_m values except for tyramine, which could be attributed to the interfere of the additional hydroxyl group. These results indicate that charged state of substrates might affect the catalyzing activity of TPAO by controlling the enzyme–substrate binding affinities upon changing pH of reaction solution.

Generally, the variability of k_{cat}/K_m values should be not much sensitive to the changes of pH. Figure 3 shows the plot of k_{cat}/K_m values against different pH, which are much smoother, more parabolic and parallel to each other

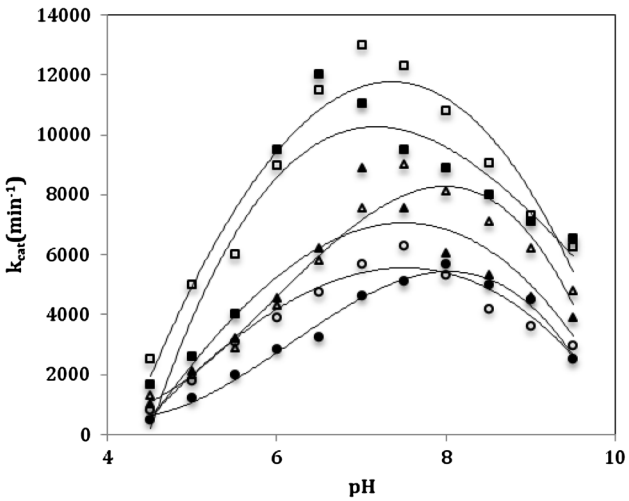

Fig. 2 Effect of pH on log k_{cat} for TPAO catalyzing different amine-containing substrates. The plots of k_{cat} against pH for different amine-containing substrates are represented by putrescine (*open square*), cadaverine (*filled square*), spermidine (*open triangle*), spermine (*filled triangle*), tyramine (*open circle*) and phenylethylamine (*filled circle*), respectively. And the *solid lines* are obtained by a nonlinear least squares fit of the plot data to Eq. 3. Experiments are carried out at 37 °C with a pH ranging from 4.0 to 9.5

compared with the curves in Fig. 1. Moreover, the corresponding pK_a values also show low degrees of variability (Table 2) compared with those derived from Fig. 2, in that free TPAO has a high ionization potential and the free amine-containing substrates are easily protonated [23].

3.3 Dependence of V_{max} and K_m on ionic strength

The effect of ionic strength (I) on the kinetic parameters of V_{max}, K_m and V_{max}/K_m was studied by using a Lineweaver–Burk equation (Eq. 4) with the same amine-containing substrates. All of the measurements were taken with

Table 2 Apparent pK_a values calculated from the pH profiles of TPAO kinetic parameters for different amine-containing substrates

Substrate	k_{cat}		k_{cat}/K_m	
	pK_{a1}	pK_{a2}	pK_{a3}	pK_{a4}
Putrescine	6.22 ± 0.11	8.04 ± 0.15	6.75 ± 0.15	8.13 ± 0.10
Cadaverine	6.53 ± 0.12	8.66 ± 0.13	7.15 ± 0.09	8.95 ± 0.12
1,8-Diaminooctane	6.82 ± 0.12	8.94 ± 0.11	7.73 ± 0.14	8.93 ± 0.12
Spermidine	6.68 ± 0.10	8.59 ± 0.13	7.26 ± 0.12	8.86 ± 0.10
Spermine	6.93 ± 0.10	8.90 ± 0.09	7.54 ± 0.14	9.01 ± 0.16
Benzylamine	7.50 ± 0.13	9.19 ± 0.17	7.61 ± 0.15	9.34 ± 0.10
Phenylethylamine	7.62 ± 0.13	9.28 ± 0.11	7.63 ± 0.16	9.30 ± 0.13
Tyramine	6.41 ± 0.12	8.39 ± 0.14	7.02 ± 0.10	8.54 ± 0.15

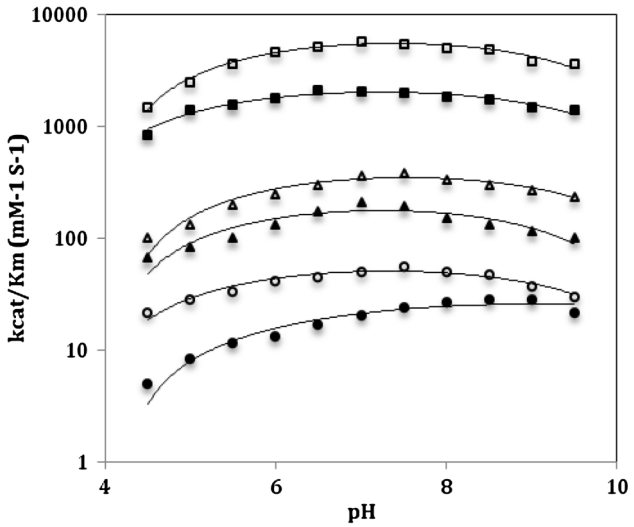

Fig. 3 Effect of pH on k_{cat}/K_m for TPAO catalyzing different amine-containing substrates. The plots of k_{cat}/K_m against *pH* for different amine-containing substrates are represented by putrescine (*open square*), cadaverine (*filled square*), spermidine (*open triangle*), spermine (*filled triangle*), tyramine (*open circle*) and phenylethylamine (*filled circle*), respectively. And the *solid lines* are obtained by a nonlinear least squares fitting. Experiments are carried out at 37 °C with a pH ranging from 4.0 to 9.5

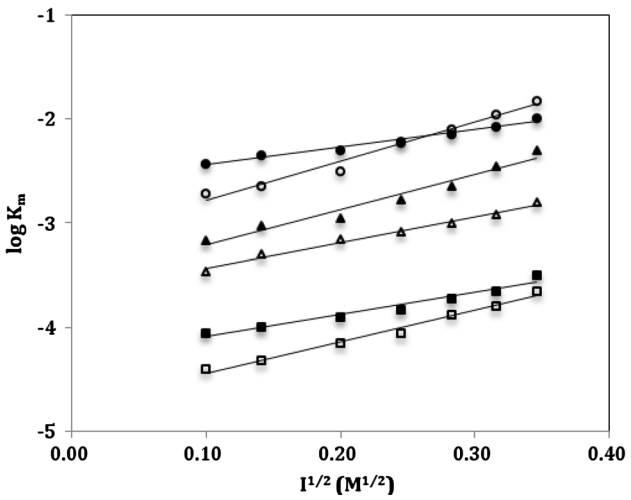

Fig. 4 Effect of ionic strength on logK_m of TPAO catalyzing different amine-containing substrates. The plots of logK_m against ionic strength ($I^{1/2}$) for different amine-containing substrates are represented by putrescine (*open square*), cadaverine (*filled square*), spermidine (*open triangle*), spermine (*filled triangle*), tyramine (*open circle*) and phenylethylamine (*filled circle*), respectively. And the *solid lines* are obtained by a nonlinear least squares fitting to Eq. 4. The correlational coefficient of 0.99 is determined for all substrates. Experiments are carried out at 37 °C, pH 7.0 and with an ionic strength ranging from 5 to 120 mM by using NaCl solution

the I ranging from 10 to 120 mM by adjusting the assay solutions with concentrated solutions of NaCl. Linear fitting curves with a correlational coefficient of 0.99 were obtained, from which the K_m (Fig. 4) and V_{max}/K_m (data not shown) values appear strongly dependent on ionic strength; in contrast, the V_{max} values (data not shown) of the tested substrates are almost independent.

The dependence of all kinetic parameters on ionic strength, the slopes ($2CZ_aZ_b$) which can be determined from the plots of log K_m against $I^{1/2}$, is given in Table 3. Among these data, the slopes derived from V_{max}/K_m fitting curves are believed to be able to reflect the interaction between substrates and enzymes. Here from Table 3, it can be clearly concluded that the ionic interaction appears with the same

Table 3 Summarized slopes ($2CZ_aZ_b$) from the plots of kinetic parameters versus $I^{1/2}$

Substrate	$2CZ_aZ_b$		
	V_{max}	K_m	V_{max}/K_m
Putrescine	−0.8 ± 0.3	+6.0 ± 0.5	−5.7 ± 0.1
Cadaverine	−0.6 ± 0.5	+6.2 ± 0.3	−5.5 ± 0.6
1,8-Diaminooctane	−0.7 ± 0.2	+5.5 ± 0.1	−5.2 ± 0.3
Spermidine	−0.4 ± 0.6	+5.1 ± 0.5	−4.1 ± 0.2
Spermine	−0.5 ± 0.7	+4.6 ± 0.4	−3.8 ± 0.5
Benzylamine	+0.2 ± 0.2	+1.8 ± 0.4	−1.9 ± 0.2
Phenylethylamine	+0.1 ± 0.3	+1.9 ± 0.7	−1.8 ± 0.5
Tyramine	+0.2 ± 0.1	+2.4 ± 0.2	−2.2 ± 0.1

order as V_{max}/K_m for different amine-containing substrates, indicating that $2CZ_aZ_b$ values depend on the relative spatial distribution of the charges present in the active site of enzymes and of those amine-containing substrates [24, 25].

Amine oxidase activities were spectrophotometrically determined at 555 nm as described by Zhang et al. in 2012. Ionic strength was determined by using NaCl with the concentrations ranging from 10 to 120 mM.

4 Discussion

AOs exist widely in different organisms and their organs; they are involved in biogenic amine metabolisms. Based on their different structural and biological functions, AOs have a physiological role in organisms. In order to understand the characterization of AOs, one must take into account that past researches were always conducted in vitro assays. In our previous publication [19], we demonstrated that an oat AO, which has exclusive substrate specificity to phenylethylamine and benzylamine, surprisingly does not have detectable activity when compared with other amines. Currently, we have carried out TPAO activity measurements under the same experimental physicochemical conditions and used different amine derivatives as substrates. During this procedure, the results indicate that diamines (putrescine and cadaverine) have the highest affinities to TPAO compared with polyamines (spermidine and spermine) and aromatic amines (phenylethylamine, benzylamine and tyramine). This behavior of TPAO appears common to AOs from other species like pea and lentil seedling [21], and soybean seedling [3].

TPAO was found to be a copper-containing diamine oxidase by Emmanuel and John [18]. A slight difference of substrate specificity of TPAO was reported in a contemporary article with respect to pea seedling amine oxidase [26] and bovine serum amine oxidase [27]. The activity of TPAO depends strongly on the carbon chain length and the structure of amines which are peaking at putrescine (C4) among diamines, spermidine (C4 + C3) among polyamines, and tyramine (phenyl + C2) among aromatic amines, all of which are measured to obtain both K_m and V_{max} values. The results indicate that the kinetic catalyzing parameters of TPAO are relatively dependent on both chemical state of the activity sites of TPAO and the structures of its substrates. Furthermore, the higher V_{max} value of spermidine compared with that of spermine could result from the fact that amino-butyl group has much higher activity than amino-propyl group to TPAO, so does the situation of putrescine and cadaverine. In order to understand the catalytic mechanism of TPAO, it should be better to resolve the active site of this enzyme by using spectroscopic and X-ray diffraction techniques.

The dependence of TPAO activity on pH is different with different amine-containing substrates. The plots of k_{cat} values versus pH display the classical bell-shaped curves (Fig. 2). The reason we selected this pH range is because that the enzyme activity is very poor beyond this range. Figure 2 suggests that the protonating and deprotonating processes are involved in recognition behaviors between substrates and enzyme activity sites. As to all of the highest values of k_{cat} from pH 6.5 to 8.0, the maximum difference was found between putrescine and phenylethylamine, which can be attributed to the polarity of substrates since phenylethylamine contains a much more nonpolar groups (phenyl-) compared with those aliphatic amines. A hypothesis that the proton interacts with both the enzyme–substrate and enzyme–product adducts due to the increased possibility of a hydrophobic site is consistent with the findings reported in previous articles [21, 28].

From the analysis of the kinetic parameters versus $I^{1/2}$, it shows that both K_m and V_{max}/K_m are significantly dependent on ionic strength. The large variability of both K_m and V_{max}/K_m indicates that electrostatic/coulomb/ionic interaction plays an important role during the substrate–enzyme docking process, in which all of the charged groups from both amine-containing substrates and the enzyme activity sites can be regulated by ionic strengths, which has already been discovered in the studies on rat mitochondrion AO [25, 29]. The ionic strength's influence actually can result from the possibility of formation on stable interaction between two negative charges of the active site with two positive charges of diamines. There are three and four nitrogen atoms for spermidine and spermine, respectively; however, there are only two positive charges on both ends of the molecular structures that could interact with two negatively charged residues in the enzyme activity site.

According to the dependence of the kinetic parameters on $I^{1/2}$, the oxidative deamination of amines by TPAO can be divided into two kinetic steps: The first one is controlled by physical factors (which regulates the formation of amine-enzyme complex by K_m), and the second step (which is controlled by chemical reactions) appears relatively independent of ionic strength because the values of the kinetic constants (V_{max}) remain relatively stable with the increasing ionic strength. The present description is consistent with the point of views of other researchers found in soybean seedling amine oxidase [24] and rat liver mitochondria matrix amine oxidase [25].

References

1. R. Angelini, A. Cona, R. Federico et al., Plant amine oxidases "on the move": an update. Plant Physiol. Biochem. **48**, 560–564 (2010). doi:10.1016/j.plaphy.2010.02.001
2. M.R. Parsons, M.A. Convery, C.M. Wilmot et al., Crystal structure of a quinoenzyme: copper amine oxidase of *Escherichia*

coli at 2 Å resolution. Structure **3**, 1171–1184 (1995). doi:10.1016/s0969-2126(01)00253-2
3. R. Medda, A. Padiglia, G. Floris, Plant copper-amine oxidases. Phytochemistry **39**, 1–9 (1995). doi:10.1016/0031-9422(94)00756-j
4. U. Bachrach, Copper amine oxidases and amines as regulators of cellular processes, in *Structure and Functions of Amine Oxidases*, ed. by B. Mondovì (CRC Press, Boca Raton/Ann Arbor/London, 1985)
5. R.D. Slocum, H.E. Flores, Polyamine catabolism in plants, in *Biochemistry and Physiology of Polyamines in Plants* (CRC Press, Boca Raton/Ann Arbor/London, 2000)
6. V. Kumar, D.M. Dooley, H.C. Freeman et al., Crystal structure of a eukaryotic (pea seedling) copper-containing amine oxidase at 2.2 Å resolution. Structure **4**, 943–955 (1996). doi:10.1016/s0969-2126(96)00101-3
7. Y. Suzuki, Purification and characterization of diamine oxidase from *Triticum aestivum* shoots. Phytochemistry **42**, 291–293 (1996). doi:10.1016/0031-9422(95)00980-9
8. A. Padiglia, R. Medda, A. Lorrai et al., Characterization of *Euphorbia characias* latex amine oxidase. Plant Physiol. **117**, 1363–1371 (1998). doi:10.1104/pp.117.4.1363
9. A. Choudhary, I. Singh, R.P. Singh, A thermostable diamine oxidase from *Vigna radiata* seedlings. Phytochemistry **52**, 1–5 (1999). doi:10.1016/s0031-9422(99)00149-1
10. B. Mondovì, A.F. Agrò, Structure and function of amine oxidases, in *Structure and Function Relationships in Biochemical Systems*, eds. by F. Bossa, E. Chiancone, A. Finazzi-Agrò, R. Strom (Springer, Boston, MA, 1982)
11. J. Planas-Portell, M. Gallart, A.F. Tiburcio et al., Copper-containing amine oxidases contribute to terminal polyamine oxidation in peroxisomes and apoplast of *Arabidopsis thaliana*. BMC Plant Biol. **13**, 13 (2013). doi:10.1186/1471-2229-13-109
12. R. Wimalasekera, C. Villar, T. Begum et al., COPPER AMINE OXIDASE1 (CuAO1) of *Arabidopsis thaliana* contributes to abscisic acid-and polyamine-induced nitric oxide biosynthesis and abscisic acid signal transduction. Mol. Plant **4**, 663–678 (2011). doi:10.1093/mp/ssr023
13. C. Hartmann, J.P. Klinman, Structure-function studies of substrate oxidation by bovine serum amine oxidase: relationship to cofactor structure and mechanism. Biochem **30**, 4605–4611 (1991). doi:10.1021/bi00232a035
14. R. Medda, A. Padiglia, J.Z. Pedersen et al., Evidence for alpha-proton abstraction and carbanion formation involving a functional histidine residue in lentil seedling amine oxidase. Biochem. Biophys. Res. Commun. **196**, 1349–1355 (1993). doi:10.1006/bbrc.1993.2401
15. A. Cona, G. Rea, R. Angelini et al., Functions of amine oxidases in plant development and defence. Trends Plant Sci. **11**, 80–88 (2006). doi:10.1016/j.tplants.2005.12.009
16. T. Kusano, T. Berberich, C. Tateda et al., Polyamines: essential factors for growth and survival. Planta **228**, 367–381 (2008). doi:10.1007/s00425-008-0772-7
17. P.N. Moschou, M. Sanmartin, A.H. Andriopoulou et al., Bridging the gap between plant and mammalian polyamine catabolism: a novel peroxisomal polyamine oxidase responsible for a full back-conversion pathway in Arabidopsis. Plant Physiol. **147**, 1845–1857 (2008). doi:10.1104/pp.108.123802
18. E. Delhaize, J. Webb, Purification and characterization of diamine oxidase from clover leaves. Phytochemistry **26**, 641–643 (1987). doi:10.1016/s0031-9422(00)84757-3
19. Y.M. Zhang, J.R. Livingstone, E. Hirasawa, Purification and characterisation of monoamine oxidase from *Avena sativa*. Acta Physiol. Plant **34**, 1411–1419 (2012). doi:10.1007/s11738-012-0939-5
20. A. Fersht, *Structure and Mechanism in Protein Science: A Guide to Enzyme Catalysis and Protein Folding* (W. H. Freeman, New York, 1999)
21. P. Pietrangeli, R. Federico, B. Mondovi et al., Substrate specificity of copper-containing plant amine oxidases. J. Inorg. Biochem. **101**, 997–1004 (2007). doi:10.1016/j.jinorgbio.2007.03.014
22. P.W. Atkins, *Physical Chemistry*, vol. 3 (Oxford University Press, Oxford, 1986)
23. B.O. Elmore, J.A. Bollinger, D.M. Dooley, Human kidney diamine oxidase: heterologous expression, purification, and characterization. J. Biol. Inorg. Chem. **7**, 565–579 (2002). doi:10.1007/s00775-001-0331-1
24. M. Luisa Di Paolo, F. Vianello, R. Stevanato et al., Kinetic characterization of soybean seedling amine oxidase. Arch. Biochem. Biophys. **323**, 329–334 (1995). doi:10.1006/abbi.1995.9957
25. R. Stevanato, S. Cardillo, M. Braga et al., Preliminary kinetic characterization of a copper amine oxidase from rat liver mitochondria matrix. Amino Acids **40**, 713–720 (2011). doi:10.1007/s00726-010-0708-y
26. A.M. Equi, A. Cooper, D.J. Robin, Chain-length dependence of the oxidation of α, ω-diamines by diamine oxidase. J. Chem. Res. Synop. **3**, 94–95 (1992)
27. M. Lunelli, M.L. Di Paolo, M. Biadene et al., Crystal structure of amine oxidase from bovine serum. J. Mol. Biol. **346**, 991–1004 (2005). doi:10.1016/j.jmb.2004.12.038
28. M.L. Di Paolo, C. Pesce, M. Lunelli et al., N-alkanamines as substrates to probe the hydrophobic region of bovine serum amine oxidase active site: a kinetic and spectroscopic study. Arch. Biochem. Biophys. **465**, 50–60 (2007). doi:10.1016/j.abb.2007.04.031
29. M.L. Di Paolo, R. Stevanato, A. Corazza et al., Electrostatic compared with hydrophobic interactions between bovine serum amine oxidase and its substrates. Biochem. J. **371**, 549–556 (2003). doi:10.1042/BJ20021055